Paper # 070RK-0017 **Topic: Reaction kinetics**

8th U. S. National Combustion Meeting
Organized by the Western States Section of the Combustion Institute
and hosted by the University of Utah
May 19-22, 2013

The Use of Dynamic Adaptive Chemistry and Tabulation in Reactive Flow Simulations

Zhuyin Ren[1] Yufeng Liu[1], Chao Xu[1], Tianfeng Lu[1], Graham M. Goldin[2]*

[1]Department of Mechanical Engineering, University of Connecticut, Storrs, CT 06269, USA
[2]ANSYS, Inc., 10 Cavendish Court, Lebanon, NH, 03766, USA

Abstract

Detailed chemical kinetics is an integral component for predictive simulation of turbulent flames and is important for reliable prediction of flames and emissions. Major challenges of incorporation of detailed chemistry in flame simulations are induced by the large number of chemical species and the wide range of timescales involved in detailed kinetics. In this work, dynamic adaptive chemistry (DAC) and in situ adaptive tabulation (ISAT) for efficient chemistry calculations in calculating turbulent reactive flows with detailed chemistry are studied in iso-octane/air homogeneous charge compression ignition (HCCI) and methane/air combustion in a partially-stirred reactor (PaSR). Chemistry calculations are accelerated by DAC via expediting the integration of ordinary differential equations (ODEs) governing chemical kinetics with local skeletal mechanisms obtained on-the-fly using the directed relation graph (DRG) method, and by ISAT via reducing the number of ODE integrations through tabulating and re-using the ODE solutions. It is shown that, in contrast to ISAT, the performance of DAC is mostly independent of the nature of combustion simulations, e.g., steady or unsteady, premixed or non-premixed combustion, and its efficiency increases with the size of chemical kinetic mechanisms. DAC is particularly suitable for transient combustion simulations with large mechanisms containing hundreds of species or more, such as those for gasoline or diesel fuels. A speedup factor of about 30 is achieved for HCCI combustion of iso-octane/air with good agreements in the histories of temperature and species concentrations. In contrast, ISAT performs better for simulations where chemistry calculations can be predominantly resolved by retrieving from the ISAT table, i.e., re-using the ODE solutions. It is shown that ISAT achieves speedup factors of about 100 with only about 10%, 0.1% and 0.01% incurred errors in NO, CO, and temperature, respectively, for the premixed methane/air PaSR simulations. Moreover, a combined DAC and ISAT approach, namely ISAT-DAC, has been developed and demonstrated in this study to accelerate chemistry evaluation. It is shown that the incurred errors in temperature and species concentrations in ISAT-DAC are well controlled, and it can significantly enhance the performance of ISAT, when the fraction of direct ODE integration is significant, via accelerating the ODE integrations by DAC.

1. Introduction

Detailed chemical kinetics is an integral component for predictive simulations of turbulent flames and is important for reliable prediction of flames and emissions. Major challenges to incorporate detailed chemistry in flame simulations are induced by the large number of chemical species and the wide range of timescales involved in detailed kinetics [1]. In this study, we consider a reacting gas-phase mixture consisting of n_s chemical species, composed of n_e elements. The thermo-chemical state of the mixture at a given location and time is determined by the pressure p, the mixture sensible enthalpy h_s, and the n_s-sized vector $\boldsymbol{Y}$ of species mass fractions. The governing equations of an inhomogeneous reactive flow can be efficiently solved by numerical schemes based on operator-splitting, which split the governing equation into sub-equations with each usually capturing only a portion of the source terms on the RHS of the governing equations. The splitted equations are time-integrated separately and assembled in the end to approximate the full equations at each

*Corresponding author:
E-mail: Zhuyin.Ren@engr.uconn.edu

time step [2-10]. With chemical reactions being separated into a single (adiabatic and isobaric) reaction fractional step, the composition $\boldsymbol{\Phi} \equiv \{\boldsymbol{Y}, h_s, p\}$ of each computational cell/particle during this sub-step evolves according to a set of nonlinear stiff ordinary differential equations (ODEs) resulting from chemical kinetics,

$$\frac{d\boldsymbol{\Phi}}{dt} = \boldsymbol{S}(\boldsymbol{\Phi}) \,, \tag{1}$$

where $\boldsymbol{S}$ is the rate of change due to chemical reactions. The task in this reaction fractional step is to determine the thermo-chemical composition due to chemical reactions over a time step Δt. The time step, typically determined by the flow field, may be constant in space and time, or a variable with a typical range spanning several orders of magnitude.

With detailed chemical kinetics, the major computational challenge is the time-intensive nature of solving Eq. (1). A realistic description of combustion chemistry for hydrocarbon fuels typically involves tens to thousands of chemical species, and the timescales can range from sub-nanoseconds to seconds [1]. In the past decade, significant progress has been made in methodologies and algorithms to reduce the computational cost imposed by the use of detailed chemistry in reactive flow simulations, and the frequently used approaches include: the development of skeletal mechanisms from large detailed mechanisms by the elimination of inconsequential species and reactions [11-18]; dimension-reduction techniques [19-29]; and storage/retrieval methodologies [30-35] such as in situ adaptive tabulation (ISAT) [33, 34]; cell agglomeration methods such as multi-zone models [36-38]; and dynamic adaptive chemistry (DAC) [14, 39-42].

The ISAT algorithm [33, 34] is currently particularly fruitful. When ISAT is employed to speedup chemistry calculations in computational fluid dynamics (CFD), which can be direct numerical simulations (DNS), large eddy simulations (LES) or a probability density function (PDF) method, the task performed by ISAT in the reaction fractional step is to determine the thermochemical compositions after a computational time step (either variable or constant) due to chemical reactions. In the context of PDF methods [43], where the system within the solution domain is represented by a large number of computational particles, the task for ISAT in the reaction step is to determine the particle compositions after a time step. By tabulating useful information in binary trees, i.e. the ISAT tables, and reusing it, ISAT can substantially reduce the number of direct chemical kinetic integrations and significantly speedup the chemistry calculations.

The computational efficiency of the ISAT algorithm is higher when the tabulated information can be re-used more frequently. For instance, speedup factors of 100~1000 can be achieved using ISAT for statistically stationary reactive flows [33]. The performance if ISAT deteriorates when the accessed composition space keeps on changing such that the pre-tabulated entries can rarely be re-used, e.g., when simulating the transient auto-ignition processes in compression ignition engines. In this study, we explore the possibility to accelerate chemistry calculation using ISAT combined with dynamic adaptive chemistry (DAC).

The DAC approach [14, 39-42] has been developed to reduce computational costs through the use of locally (spatially and temporally) valid skeletal mechanisms. DAC involving on-the-fly chemical mechanism reduction for accelerating chemistry calculations has been demonstrated in internal combustion engine (ICE) simulations [14, 39-41]. In a recent turbulent reactive flow simulation [42], DAC is achieved through the directed relation graph (DRG) method [11, 12], which was invoked for each CFD cell to obtain a small skeletal mechanism that is valid for the local thermochemical condition. By doing so, only a small subset of species and reactions in the full mechanism were retained to capture the dominant reaction pathways for each local condition. Consequently, the ODE system governing chemical kinetics during the reaction fractional step is reduced in size due to the eliminated unimportant species.

In the present study, we first investigate the relative performance of DAC and ISAT in simulating both premixed and non-premixed methane/air combustion in a partially-stirred reactor (PaSR) and in simulating a homogeneous charge compression ignition (HCCI) combustion of iso-octane/air mixtures. Then the methodology and test results, including the reduction in simulation time and the loss in accuracy, for the combined use of DAC and ISAT for efficient chemistry calculations are reported. As an outline of the paper, the ISAT algorithm and the DAC approach will be reviewed in Section 2. Their relative performances in

PaSR and HCCI are studied in Section 3. The integration of DAC and ISAT is formulated and investigated in Section 4. Conclusions are presented in Section 5.

2. Methods

2.1 Overview of the ISAT algorithm

The purpose of ISAT is to tabulate a function $\boldsymbol{f}(\boldsymbol{x})$, where $\boldsymbol{x}$ and $\boldsymbol{f}$ are of dimensions n_x and n_f, respectively. Given a query with $\boldsymbol{x}^q$ as input, ISAT returns $\boldsymbol{f}^a(\boldsymbol{x}^q)$ as an approximation to $\boldsymbol{f}(\boldsymbol{x}^q)$ if possible. An essential aspect of ISAT is that the table is built-up *in situ*, or at runtime, as the simulation is being performed, not in a pre-processing stage. The table is empty at the beginning of the simulation. Table entries, also referred to as leaves, are added as needed based on the queries, $\boldsymbol{x}^q$, generated by the simulation. As such, only the compositions accessed during the simulation need to be tabulated. The tabulated information on the n-th leaf includes its location, $\boldsymbol{x}^{(n)}$, the function value, $\boldsymbol{f}^n=\boldsymbol{f}(\boldsymbol{x}^{(n)})$, and the $n_f \times n_x$ Jacobian matrix, $\boldsymbol{A}^{(n)}$, defined as $A_{ij} = \partial f_i/\partial x_j$The $\boldsymbol{A}$ matrix is used to construct the linear approximation employed in ISAT. Given a query, $\boldsymbol{x}^q$, the linear approximation to $\boldsymbol{f}(\boldsymbol{x}^q)$ on the n-th leaf is

$$\boldsymbol{f}^{l,n} = \boldsymbol{f}^n + \boldsymbol{A}^{(n)}(\boldsymbol{x}^q - \boldsymbol{x}^n), \tag{2}$$

and the error in this approximation is

$$\varepsilon^{(n)}(\boldsymbol{x}^q) = \left\|\boldsymbol{f}^{l,n}(\boldsymbol{x}^q) - \boldsymbol{f}(\boldsymbol{x}^q)\right\|. \tag{3}$$

It is assumed that $\boldsymbol{f}$ and $\boldsymbol{x}$ are normalized, such that the two-norm is an appropriate measurement of the approximation error. Given a small error tolerance,ε_{ISAT} , ISAT returns an approximation to $\boldsymbol{f}(\boldsymbol{x})$ with errors, ε, which are (with reasonable probability) less than ε_{ISAT}. An important concept related to the approximations above is the region of accuracy (ROA) of a leaf. The ROA of the n-th leaf is defined as a domain that contains $\boldsymbol{x}^{(n)}$, at each point within which the error $\varepsilon^{(n)}(\boldsymbol{x})$ in the linear approximation is less than the specified error tolerance, ε_{ISAT}. In ISAT, the ROA is approximated by an ellipsoid, namely the ellipsoid of accuracy (EOA). The EOA is initialized conservatively and may grow as additional information becomes available. Note that both the ISAT storage requirement and the retrieval timescale with n_x^2, with $n_x \approx n_f$.

ISAT has been widely used to efficiently incorporate reduced or detailed chemical kinetic mechanisms in CFD calculations of turbulent reactive flows [43-45]. In these applications, $\boldsymbol{x}$ consists of the thermochemical state of a computational particle/cell at the beginning of the reaction time step of duration Δt, and $\boldsymbol{f}$ represents the composition at the end of the integration step at adiabatic and isobaric condition. Evaluating $\boldsymbol{f}(\boldsymbol{x})$ involves integrating the set of n_f stiff ODEs in Eq. (1) for a time Δt. The basic operations performed by ISAT on a query, $\boldsymbol{x}^q$, are summarized in the following:

1. Retrieval: If the query point falls within the ellipsoid of accuracy (EOA) of $\boldsymbol{x}$, the linear approximation to $\boldsymbol{f}(\boldsymbol{x}^q)$ based on that leaf is returned. This operation is denoted as a "retrieve".
2. Growth: If a retrieval attempt failed, $\boldsymbol{f}(\boldsymbol{x}^q)$ is directly evaluated and returned. Some leaves close to $\boldsymbol{x}^q$ are selected for growth attempts. For each of these selected leaves, the error $\boldsymbol{\varepsilon}$ in the linear approximation to $\boldsymbol{f}(\boldsymbol{x}^q)$ is evaluated, and if it is less than ε_{ISAT}, the leaf's EOA is grown to cover $\boldsymbol{x}^q$. If at least one growth attempt is successful, this operation is called a "grow".
3. Addition: If none of the leaves close to $\boldsymbol{x}^q$ can be grown to achieve an error smaller than ε_{ISAT} and the table is not full, i.e., the ISAT table has not reached the allowed memory limit, a new leaf associated with $\boldsymbol{x}^q$ is added to the ISAT table. This operation is called an "add".
4. Discarded evaluation: If an "add" attempt cannot be completed because the ISAT table is full, $\boldsymbol{f}(\boldsymbol{x}^q)$ obtained by the function evaluation is returned without further action. (Hence the function evaluation has no effect on the ISAT table.) This operation is called a "discard".

Note that one event of grow, add, or discarded evaluation involves one and only one ODE integration. The average CPU time to perform an ODE integration, denoted as t_F, is typically several orders of magnitude larger than the average CPU time to perform a "retrieve", denoted as t_R. ISAT speeds up the chemistry calculations by obtaining the reaction mapping using "retrieve" whenever possible. Its performance depends on the fraction of function evaluation p_F in a simulation, which is defined to be the sum of the probabilities of "grow", "add", and "discard". In a simulation, the fractions of different events depend on the allowed number

of table entries, the number of queries performed, and the nature of the simulation. With p_R being the fraction of "retrieve", the average CPU time for a query, t_Q, to a good approximation, is

$$t_Q = t_R p_R + t_F p_F = t_R(1 - p_F) + t_F p_F, \tag{4}$$

and the speedup factor in chemistry calculation is

$$\gamma = \frac{t_F}{t_Q} = \frac{1}{p_F + (1 - p_F) t_R / t_F}. \tag{5}$$

With ISAT, the ideal speedup factor is $\gamma = t_F / t_R$, that occurs when p_F approaches zero, i.e., almost all the compositions can be resolved by "retrieve". In contrast, the ISAT performance deteriorates for simulations where p_R approaches unity.

2.2 **Overview of dynamic adaptive chemistry**

Dynamic chemistry adaption (DAC) can be achieved through the DRG-based methods [11-14], which is invoked for each CFD cell/particle to obtain a small skeletal mechanism that is valid for the local thermochemical condition. More specifically, given a specific thermochemical state $\boldsymbol{\Phi} \equiv \{\boldsymbol{Y}, h_s, p\}$, DRG is invoked to eliminate the unimportant species and the involved reactions in the mechanism that have negligible effects on the retained species. The method of DRG is based on the observation that many species are only weakly coupled during combustion processes, such that the species that do not significantly affect the reaction rates of the major species can be eliminated from the mechanism. The first step in DRG is to quantify species coupling by the pair-wise error, r_{AB}, induced to a species *A* by the elimination of another species *B* for a given thermochemical state [46]:

$$r_{AB} \equiv \frac{\max_i |\nu_{A,i}\, \omega_i \delta_{Bi}|}{\max_i |\nu_{A,i} \omega_i|}, \quad \delta_{Bi} = \begin{cases} 1, \text{if the ith reaction involves B} \\ 0, \text{otherwise} \end{cases}, \tag{6}$$

where $\omega_i$is the net reaction rate of the *i*-th reaction and $\nu_{A,i}$ is the stoichiometric coefficient of species *A* in the *i*-th reaction. It is seen that the denominator in Eq. (6) indicates the maximum flux contribution for the creation and consumption of species *A*, while the numerator indicates the maximum flux of *A* that involves species *B*. Therefore, a small r_{AB} indicates that *B* is not important for the reaction rate of species *A*. Otherwise *B* is important to *A* and should be retained in the skeletal mechanism if *A* is retained. Once the pair-wise species reduction errors are quantified, the species dependence defined based on Eq. (6) can then be expressed in the following graph notation

$$A \to B \;\; if \; r_{AB} > \varepsilon_{DAC}, \tag{7}$$

i.e., there is a directed edge from species *A* to *B* if and only if r_{AB} is larger than a pre-specified reduction threshold ε_{DAC}. The vertices in the DRG are the species in the detailed mechanism, and the adjacency matrix, $\boldsymbol{E}$, of the digraph can be constructed as:

$$A = \begin{cases} 1, if \; r_{ij} > \varepsilon_{DAC} \\ 0, if \; r_{ij} \le \varepsilon_{DAC} \end{cases}, \tag{8}$$

In addition to the reduction threshold, the DRG method requires as input one or more species (e.g., major species, important radicals and/or other species of interest) as the search-initiating, or starting species (together with matrix $\boldsymbol{E}$) to determine the important species to be retained in the skeletal mechanism. Starting from these species of interest, the Depth-First Search (DFS) algorithm can be employed to identify all the species that are strongly coupled to the starting species. DRG is a linear time reduction algorithm and has been employed to obtain skeletal mechanisms for various detailed mechanisms. In previous studies [14, 39-42], the starting species are manually specified, e.g. to include the fuel components together with *CO*, *H* and *NO* [42]. In this study, with a given local composition, the *M*-1 most abundant species (in mass) together with species *H* are chosen to be the *M* search-initiating species, where *M* is a user-specified small integer. This automatic procedure works well for different fuels as demonstrated in the following tests.

In CFD calculations of reactive flows with DAC, the full set of chemical species in a detailed chemical kinetic mechanism are transported in the governing equations. At the beginning of each reaction fractional step, DRG is invoked for each CFD cell/particle to obtain a small skeletal mechanism that is valid for the local thermochemical condition based on a pre-specified reduction error threshold. The ODEs in Eq. (1) for the unimportant species are simplified by approximating these species to be chemically frozen during the integration time step, i.e. a reaction is excluded from the local skeletal mechanism if it involves any

unimportant species as reactants or products. Note that the eliminated species may still act as third-bodies. Next, the simplified ODEs are integrated for a reaction time step to obtain the composition after the reaction fractional step. The computation time saving by using DAC is achieved by solving only the non-trivial ODEs in Eq. (1) during the reaction fractional steps.

3. Results and discussions

Since neither ISAT nor DAC requires pre-processing or pre-tabulation of sample compositions, both methods are particularly suitable for flame simulations in which a wide range of thermochemical conditions are involved. Furthermore, both methods have been successfully demonstrated to speedup chemistry calculations in combustion applications. In the present study, the relative performance of DAC and ISAT is further investigated and compared in PaSR and HCCI engine simulations to characterize the dependence of their performances on the natures of different combustion simulations, e.g., at steady or unsteady, premixed or non-premixed conditions. Simulations are performed with and without DAC and/or ISAT to quantify and compare the incurred errors in temperature and species concentrations, primarily *CO* and *NO*, which are important intermediate species for fuel oxidation and emissions. The time savings achieved with DAC and ISAT are also reported.

3.1 Test case: PaSR

To demonstrate the feasibility and efficiency of DAC and ISAT for turbulent combustion simulations, PaSR calculations were performed for both premixed and non-premixed combustion of methane/air with the 53-species GRI-Mech 3.0 [47] and 129-species USC-Mech II with updated NOx pathways [48, 49], respectively. A PaSR is similar to an individual grid cell in a PDF simulation of a turbulent reacting flow [43]. A stochastic PaSR simulation involves N_p particles at any time, t, with Δt being the specified integration time step. At each discrete temporal location $k\Delta t$, where k is an integer, the particle compositions change discontinuously corresponding to inflow and outflow. Between these discrete temporal points, the particle compositions can be changed by mixing and chemical reactions, which are solved using the operator-splitting scheme. The particles are arranged in pairs: particles 1 and 2, 3 and 4,…, N − 1 and N are partners. The mixing fractional step for each pair of particles, say p and q, is governed by

$$\begin{cases} d\boldsymbol{\Phi}^{(p)}/dt = -(\boldsymbol{\Phi}^{(p)} - \boldsymbol{\Phi}^{(q)})/\tau_{mix} \\ d\boldsymbol{\Phi}^{(q)}/dt = -(\boldsymbol{\Phi}^{(q)} - \boldsymbol{\Phi}^{(p)})/\tau_{mix} \end{cases}, \tag{9}$$

where $\tau_{mix}$is a specified mixing timescale for the pair-wise mixing process. In the reaction fractional step, each particle evolves independently as described by Eq. (1). With τ_{res} being the specified residence time, outflow and inflow consist of selecting $\frac{1}{2}N_p\Delta t/\tau_{res}$ pairs at random and replacing their compositions with inflow compositions, which are drawn from a specified distribution. With τ_{pair} being the specified pairing timescale, $\frac{1}{2}N_p\Delta t/\tau_{pair}$ pairs of particles (other than the inflowing particles) are randomly selected for pairing. Then these particles and the inflowing particles are randomly shuffled so that (most likely) they change partners.

For the premixed cases, the PaSR involves two inflowing streams: a stoichiometric premixed stream of fresh fuel/air mixture at 600*K*, and a pilot stream consisting of the adiabatic equilibrium products of the stoichiometric fuel/air mixture at an initial temperature of 600*K*. The mass flow rates of the fresh and pilot streams are in the ratio of 0.95:0.05. For the non-premixed cases, the PaSR involves three inflowing streams: a stream of pure fuel at 300*K*, a stream of air at 300*K*, and a pilot stream consisting of the adiabatic equilibrium products of the stoichiometric fuel/air mixture at an initial temperature of 300K. The mass flow rates of these three streams are in the ratio of 0.05:0.85:0.10. For both the premixed and non-premixed cases, all the initial particle compositions at t = 0 are set to be those of the corresponding pilot-streams. Pressure is atmospheric for all the PaSR simulations. Other important parameters involved in the PaSR simulations are listed in Table 1, including residence time, τ_{res}, mixing timescale, τ_{mix}, pairing timescale, τ_{pair}, time step, Δt, and number of particles, N_p. These PaSR parameters are chosen to produce a good range of temperature and species compositions to effectively mimic non-equilibrium combustion processes with strong turbulent-chemistry interactions. In particular, as the residence time decreases and approaches the blow-out limit, ISAT

and DAC will be assessed over the dramatically varying composition space at near-limit conditions. All the PaSRs are simulated for time duration of $10\tau_{res}$ to reach statistically stationary. The maximum size of the ISAT tables is set to be 500MB for all the PaSR simulations.

Table 1: The PaSR parameters used for the test cases for methane/air.

Parameters	τ_{res}	τ_{mix}	τ_{pair}	N_p	Δt
Non-premixed	15ms	1ms	1ms	1000	0.1ms
Premixed	5ms	1ms	1ms	1000	0.1ms

Figure 1 shows the evolution of the mean temperature and *NO* mass fractions in the premixed PaSR with the 129-species USC-Mech II. As indicated by the variations in temperature and NO concentration, a wide range of non-equilibrium conditions in the composition space was involved in this test case. The error threshold for the simulations with DAC is $\varepsilon_{DAC} = 0.01$, and that with ISAT is $\varepsilon_{ISAT} = 5 \times 10^{-6}$. It is seen that the mean temperature profiles with DAC or ISAT closely follow that without DAC or ISAT with no visible differences, while minor discrepancies are present in the mean NO concentration profiles. Improved agreements with the exact description can be achieved with reduced ε_{DAC} for DAC and reduced ε_{ISAT} for ISAT since both ISAT and DAC have effective accuracy control in temperature and species concentrations.

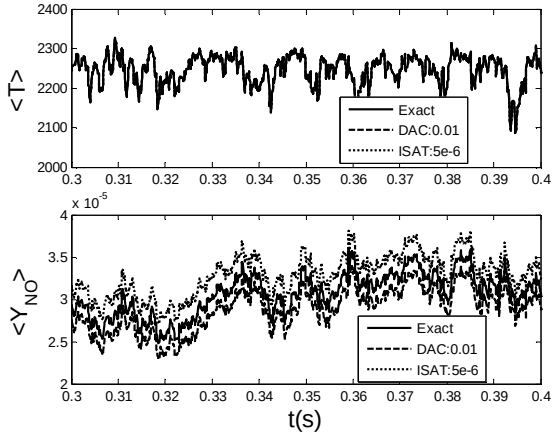

Figure 1. The evolution of the mean temperature (K) and mean NO mass fraction in the PaSR for the premixed case with the 129-species USC-Mech II.

To further quantify the accuracy, we measured the mean relative percentage errors incurred in temperature and species concentrations (CO and NO) over the entire simulation. The relative percentage error is defined as

$$\varepsilon_{\psi} = \frac{|\psi^{ID} - \psi^{E}|}{\psi^{ID} + \psi^{E}} \times 100, \tag{10}$$

where ψ is a quantity of interest, e.g., temperature or a species concentration, $\psi^{ID}$is the predicted value with ISAT or DAC, and $\psi^{E}$is the exact solution without the ISAT or DAC.

Figure 2 compares the relative errors of ISAT and DAC in temperature and *CO* and *NO* concentrations as functions of the speedup factor for DAC and ISAT for the premixed case. The speedup factor is computed based on the entire simulation time, rather than the CPU time for chemistry integration. The ratio of the CPU time spent on the physical processes not including chemical reactions (e.g., inflow/outflow and the mixing process) and that on chemistry calculations without acceleration strategies is 1:380 using USC-Mech II and 1:120 using GRI-Mech 3.0. In the simulations with ISAT, more than 98% of the particle compositions are resolved by retrieving from the ISAT table, and thus high speedup factors were achieved as shown in Fig. 2, where the data points located in the lower-right corner indicate higher efficiencies with smaller errors. It is further observed in Fig. 2 that

- When almost all the compositions can be resolved by retrievals, ISAT is much more efficient than DAC. It is seen in Fig. 2 that ISAT achieves speedup factors of about 100 with only about 10%, 0.1% and 0.01% incurred errors in *NO*, *CO*, and temperature, respectively. In contrast, with the same levels of

incurred errors, the speedup factors achieved by DAC are less than 10 even with the 129-species USC-Mech II.

- The speedup factor achieved by DAC significantly increases with the mechanism size, i.e., the number of species, whereas that of ISAT is mostly insensitive to the mechanism size. For instance, DAC achieved a speedup factor of about 8 with about 10%, 0.3% and 0.03% incurred errors in *NO*, *CO*, and temperature, respectively, using USC-Mech II, while only a speedup factor of about 2 was achieved using GRI-Mech 3.0 at the same levels of incurred errors. This is because the 129-species USC-Mech II has a larger room for reduction compared to the 53-species GRI-Mech 3.0, since the latter is rather compact for methane oxidation. This point is confirmed in Fig. 3, which shows the mean fraction of retained species rr_{spe} and reactions rr_{rxn} by DRG with $\varepsilon_{DAC} = 0.1$. It is seen that reductions by factors of about 85% and 90% were achieved in the number of species and reactions, respectively, using USC-Mech II, while only factors of about 65% and 75% were achieved using GRI-Mech 3.0.

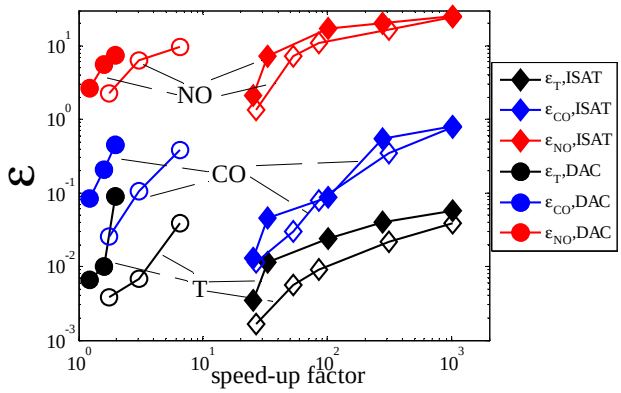

Figure 2. The incurred relative percentage errors in temperature (black symbols), CO (blue symbols) and NO (red symbols) as functions of the speedup factor for DAC and ISAT for the premixed PaSR. Closed symbols: with GRI-Mech 3.0; Open symbols: with USC-Mech II. The symbols are obtained with different values ofε_{DAC} or ε_{ISAT}.

In the present study, during the numerical integration of the ODEs Eq. (1), Jacobian of the reaction source term is evaluated through the time consuming numerical perturbations along the reaction trajectory. As such, the computational cost in ODE integration is approximately proportional to n_s^2. Since both the retrieval time t_R and the ODE integration time t_F scale with n_s^2, as indicated by Eq. (5), the performance of ISAT consequently does not depend on the size of mechanism (when the fraction of ODE integration remains unchanged).

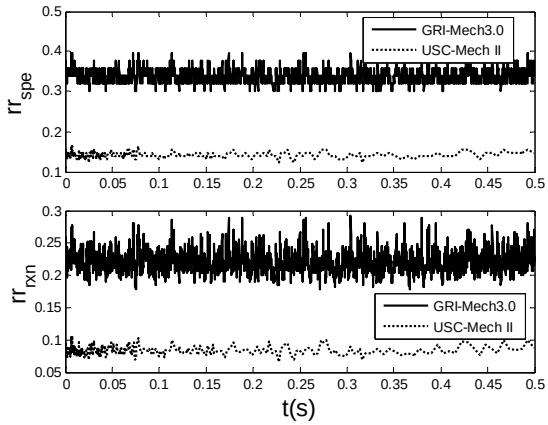

Figure 3. The mean fraction of retained species, rr_{spe} and reactions, rr_{rxn} by DRG with $\varepsilon_{DAC} = 0.1$for the premixed PaSR.

To further show the performance of DAC and ISAT for non-premixed combustion, Fig. 4(a) shows the evolution of the mean temperature for the non-premixed PaSR with the 129-species USC-Mech II. The

error tolerances were set to be $\varepsilon_{ISAT} = 2 \times 10^{-5}$and $\varepsilon_{DAC} = 0.01$ for ISAT and DAC, respectively. As indicated by the larger-than-600K variations in the mean temperature, a wide range of compositions are present in this test case. It is seen that the solutions with either ISAT or DAC are accurate compared with the exact solution for this rather challenging case, and there are almost no noticeable errors in the mean temperature profiles. Figures 4(b) and (c) show the evolutions of the mean concentrations of *CO* and *NO*. For the simulation with ISAT, while the errors are small in temperature and *CO* concentration, larger errors were observed for the mean *NO* concentration, showing that the level of incurred error can depend on the quantity of interest.

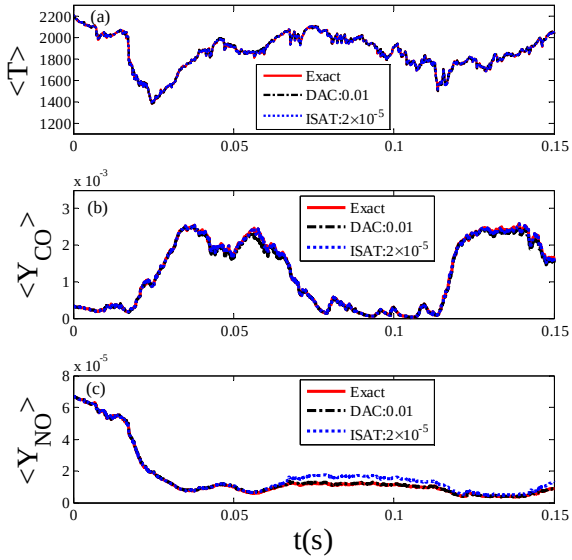

Figure 4. The evolution of [(a)] the mean temperature (K), [(b)] mean *CO* mass fraction, and [(c)] mean *NO* mass fraction in the non-premixed PaSR with the 129-species USC-Mech II.

It is noted that this non-premixed PaSR is computationally more challenging for ISAT than the premixed case, as indicated by the fractions of "retrieve" shown in Table 2. For instance, the retrieval rate is only 38% for the non-premixed case, while it is more than 98% for the premixed case with$\varepsilon_{ISAT} = 2 \times 10^{-5}$. Consequently, the speedup factors achieved for the non-premixed PaSR are less than 3 as shown in Fig. 5, which are significantly smaller than those in the premixed cases due to the increased computational time for direct chemistry integrations. Figure 5 further shows that comparable computational efficiency were achieved for the non-premixed PaSR using ISAT and DAC, respectively. More interestingly, to achieve the same speedup factor, ISAT incurs smaller errors in temperature and *CO* concentration and larger errors in *NO* concentration than those by DAC. For instance, with a speedup factor of 3, ISAT incurs about 25%, 0.9% and 0.1% incurred errors in *NO*, *CO*, and temperature, respectively, while those by DAC are approximately 9%, 9% and 0.3%, respectively.

Table 2: The fraction of "retrieve" for the non-premixed PaSR with USC-Mech II.

ε_{ISAT}	1×10^{-4}	5×10^{-5}	2×10^{-5}
p_R	75%	55%	38%

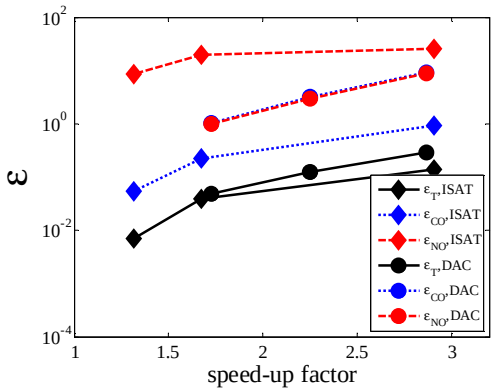

Figure 5. Incurred errors in temperature, *CO* and *NO* concentrations as functions of the speedup factor for simulations with DAC or ISAT for the non-premixed PaSR with USC-Mech II. The results using DAC were obtained with ε_{DAC}=0.01, 0.1, 0.2 respectively, and those with ISAT were obtained with $\varepsilon_{ISAT} = 2 \times 10^{-5},\ 5 \times 10^{-5}, 1 \times 10^{-4}$, respectively.

3.2 **Test case: HCCI**

In HCCI combustion [50] premixed charges of fuel-air mixtures are compressed until auto-ignition occurs. HCCI combustion has received substantial research interest due to its potential benefits of high thermal efficiency and low engine-out *NOx* and soot emissions, due to the overall low flame temperatures resulting from the lean combustion of nearly homogeneous fuel/air mixtures. These benefits make HCCI engine an attractive alternative for the conventional internal combustion engines.

In the present study, an HCCI combustion test is designed to illustrate the performance of DAC for transient compression ignition processes involving complex fuel chemistry of the iso-octane/air mixture with equivalence ratio of 0.2. The initial temperature is set to be 850K at 30 crank-angle-degree (CAD) before the top dead center (TDC), and the initial pressure is 13.6 atm. The fuel chemistry is described by an 874-species iso-octane detailed mechanism [51]. The cylinder volume evolves with time and temperature peaks close to TDC. The engine speed is 1000 rpm. The governing equations are solved by an operator-splitting scheme, which separates the time-integration of the compression/expansion process and chemical reactions into two sub-steps. The reaction sub-step is taken to be isobaric. After the reaction sub-step, pressure is adjusted such that the system contains the same amount of mass as that before the reaction sub-step. The integration time step size is fixed at $\Delta t = 1 \times 10^{-6} s$.

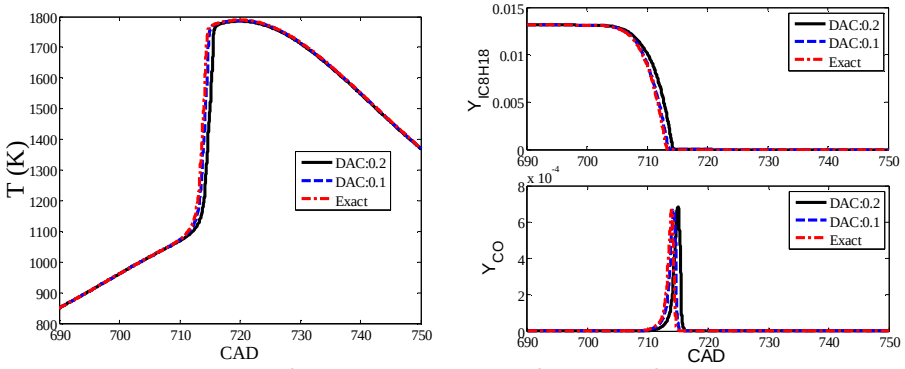

Figure 6. Temperature and concentrations of iso-octane and CO as functions of CAD calculated with different reduction threshold values for the HCCI combustion of the iso-octane/air mixture with an equivalence ratio of 0.2.

Figure 6 compares the profiles of temperature and species concentration histories calculated with and without DAC. Different reduction threshold values were used to investigate the error control of DAC. The mixture ignites at around 8 CAD before TDC. It is seen that the results calculated with DAC approach the exact solution, i.e. the full description without DAC, as the reduction threshold, ε_{DAC}, decreases, implying

that DAC has an effective accuracy control for the HCCI simulation. The difference in the ignition point, which is taken to be the crank angle where temperature reaches 1100K, between the solutions with and without DAC is less than 0.2 CAD for $\varepsilon_{DAC} = 0.1$ and 1 CAD for $\varepsilon_{DAC} = 0.2$ respectively. At the same time, DAC resulted in significant reduction in the simulation time. Speedup factors of 18 and 32 were achieved with $\varepsilon_{DAC} = 0.1$ and $\varepsilon_{DAC} = 0.2$, respectively.

Figure 7 further shows the fraction of species retained by DRG as a function of CAD in the HCCI simulation. It is seen that the extent of reduction achieved by DRG strongly depends on the combustion states. During the compression and ignition stage (before approximately 715 CAD), where the radicals proliferate and ignition consequently occurs, the fraction of retained species is approximately 10% and 15% for the simulations with $\varepsilon_{DAC} = 0.2$ and $\varepsilon_{DAC} = 0.1$, respectively. After 725 CAD, where the mixture has ignited and mostly reached chemical equilibrium, the fraction of important species retained reduces to about 0.02. That is, only about 20 species are important at the late stage of expansion. It is further observed that the fraction of retained species fluctuates slightly at the late stage of expansion. This is because the mixture composition used for DRG reduction may deviate from the intrinsic low-dimension manifold of the reactive system in the compression/expansion stage, such that some unimportant species may be reactivated. Furthermore, at the near-equilibrium stage, exhausted chemical reactions may also be reactivated by the numerical errors in the operator-splitting scheme.

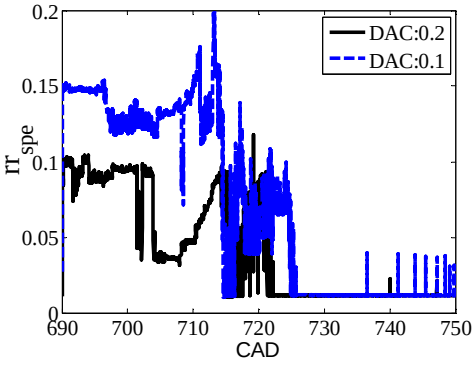

Figure 7. The mean fraction of species retained by DRG, rr_{spe}, as a function of CAD for the HCCI combustion of the iso-octane/air mixture with an equivalence ratio of 0.2.

It is further noted that for this HCCI test case, ISAT resulted in little reduction in computational time since the thermo-chemical states of the system keep on evolving in the composition space such that the table entries can rarely be re-used.

3.3 **Discussions**

As demonstrated above, both ISAT and DAC can achieve significant computational time savings in chemistry calculations with effective error control. The performance of DAC is almost independent of the nature of combustion systems, e.g., both premixed and non-premixed, and its computational efficiency increases with the mechanism size. Therefore, DAC is particularly suitable for simulations of transient combustion processes with large mechanisms, particularly those for practical engine fuels that may involve hundreds of species or more. In contrast, ISAT performs better for statistically stationary flames, where the compositions can be frequently retrieved from the ISAT table. Since the storage requirement and the retrieval time in ISAT scale with $n_s{}^2$, ISAT is most effective for moderate sized mechanisms, e.g., those with less than about 50 species. The performance of ISAT deteriorates when the tabulated reaction states can rarely be retrieved, e.g. in transient combustion simulations. In the following, DAC will be combined with ISAT for improved performance through expediting the time-integration of Eq. (1).

4. ISAT-DAC for highly efficient combustion simulations

The method with combined ISAT and DAC approach, denoted as ISAT-DAC, for the reaction sub-step of a CFD simulation is shown in Fig. 8. The composition, $\boldsymbol{\Phi} \equiv \{\boldsymbol{Y}, h_s, p\}$, to be solved in CFD, with DNS, LES, or PDF methods, typically involve the full set of chemical species in a detailed chemical kinetic mechanism.

During the reaction sub-step with ISAT-DAC, the composition $\boldsymbol{\Phi}(\Delta t)$ is determined based on the starting composition $\boldsymbol{\Phi}(0)$ at adiabatic and isobaric conditions. An ISAT table stores the pair of values of $\boldsymbol{\Phi}(0)$ and $\boldsymbol{\Phi}(\Delta t)$ to be re-used in future integration steps. If needed, new table entries can be inserted *in situ* through the following procedure:

- Given the initial composition $\boldsymbol{\Phi}(0)$, DRG reduction is performed to obtain a skeletal mechanism that is valid for the local thermochemical condition.
- The simplified ODEs for the species retained in the skeletal mechanism are integrated for a time step, Δt, to obtain the full composition, $\boldsymbol{\Phi}(\Delta t)$, in which the unimportant species are approximated to be frozen.
- The $(n_r + 1) \times (n_r + 1)$ sensitivity matrix, defined as $A_{ij}^r = \partial \phi_i^r(\Delta t)/\partial \phi_j^r(0)$, for the reduced system is obtained from the ODE solver, e.g. DDASAC [52]. In the present approach, the ISAT operations, such as "retrieve", are performed based on the full composition. The required $(n_s + 1) \times (n_s + 1)$ full gradient matrix $A_{ij} = \partial \phi_i(\Delta t)/\partial \phi_j(0)$ is obtained based on $\boldsymbol{A}^r$ by neglecting the sensitivities of the retained species with respect to the unimportant species and including the columns of the $(n_s + 1) \times (n_s + 1)$ identity matrix corresponding to the unimportant species index.

It is found in numerical tests that the above procedure incurs significant errors when retrieving from the table due to the inaccuracy in the sensitivity matrices since the sensitivities of the retained species with respect to the unimportant species are not taken into account. Due to this observation, the above process is revised so that only until the table is full, DAC is invoked to expedite the ODE integrations. That is the full mechanism is used when building up the table and no approximations of the sensitivities are made.

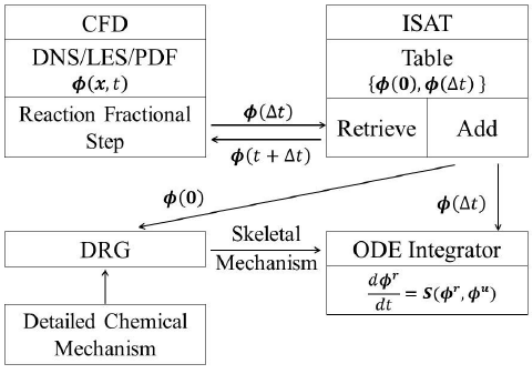

Figure 8. Schematic of ISAT-DAC employed in the reaction sub-step.

The ISAT-DAC method inherited the advantages from both ISAT and DAC to efficiently solve combustion problems with complex chemistry: The number of expensive direct ODE integrations is reduced by tabulating and reusing the solutions, and the required direct integrations after the table is full are expedited by the local DRG reduction. Similar to ISAT, the table in ISAT-DAC is built up *in situ* as the simulation being performed. In the present implementation of ISAT-DAC, both the storage requirement for ISAT and the retrieval time scale with $(n_s + 1)^2$, since "retrieve" and "add" are performed in the full composition space.

Figure 9 shows the incurred errors in temperature and concentrations of *CO* and *NO* as functions of the ISAT error tolerance for the non-premixed PaSR calculated with USC-Mech II. In the ISAT-DAC approach, the reduction threshold is set to be $\varepsilon_{DAC} = 0.01$. It is seen that the ISAT error tolerance effectively controls the percentage errors incurred with the ISAT-DAC method in predicted temperature and species concentrations for the given reduction threshold value. With $\varepsilon_{ISAT} = 2 \times 10^{-5}$, the incurred relative errors by ISAT-DAC are less than 0.05% in temperature, 0.9% in *CO*, and 10% in *NO*, which are comparable to those using DAC alone with $\varepsilon_{DAC} = 0.01$. Figure 10 illustrates the relative performance of the stand-alone ISAT and the ISAT-DAC methods. As shown, for the same speedup factor, the ISAT-DAC method achieves better accuracy in temperature and *NO* concentration than that of the stand-alone ISAT method. For instance, with a speedup factor of two, the stand-alone ISAT incurs about 20% error in *NO* concentration whereas ISAT-DAC incurs only about 9% error.

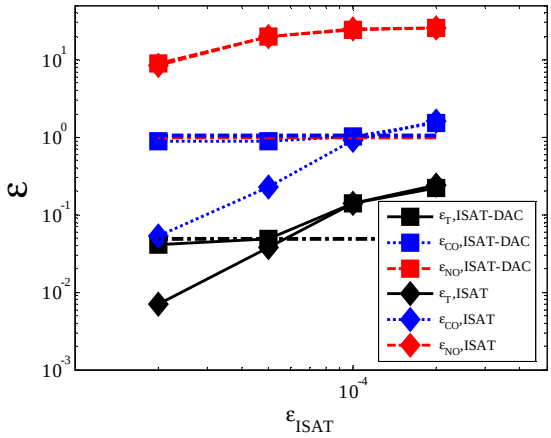

Figure 9. The incurred errors in temperature and concentrations of *CO* and *NO* as functions of the ISAT error tolerance for the non-premixed PaSR with USC-Mech II. The reduction threshold is $\varepsilon_{DAC} = 0.01$ in ISAT-DAC. The horizontal dash-dot lines represent the incurred errors from the stand-alone DAC method with $\varepsilon_{DAC} = 0.01$.

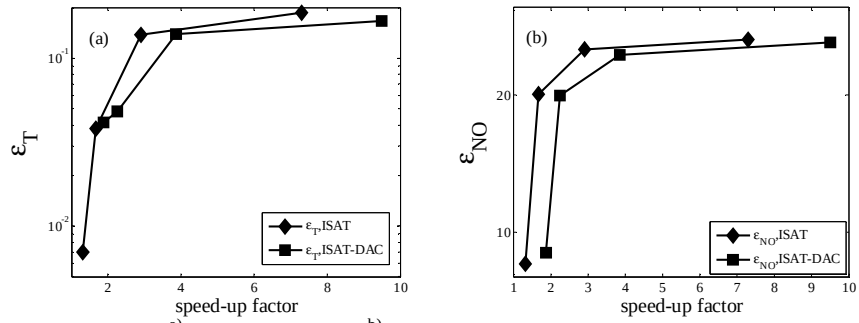

Figure 10. The incurred errors in [a] temperature and [b] *NO* concentration as functions of the speedup factor for the non-premixed PaSR with USC-Mech II. The data points are obtained with $\varepsilon_{ISAT} = 2 \times 10^{-5}$, 5×10^{-5}, 1×10^{-4}, 1.5×10^{-4}, respectively for both ISAT and ISAT-DAC. In ISAT-DAC, the reduction threshold is $\varepsilon_{DAC} = 0.01$.

To further quantify the computational efficiency, Table 3 summarizes the speedup factors achieved by ISAT and ISAT-DAC, respectively. As shown, with the same value of ε_{ISAT}, ISAT-DAC (with $\varepsilon_{DAC} = 0.01$) is 30% more efficient than the stand-alone ISAT for the non-premixed PaSR with USC-Mech II.

Table 3. The speedup factors (SF) achieved by in ISAT and ISAT-DAC for the non-premixed PaSR with USC-Mech II. The reduction threshold in ISAT-DAC is $\varepsilon_{DAC} = 0.01$.

ε_{ISAT}	2×10^{-5}	5×10^{-5}	1×10^{-4}	1.5×10^{-4}
SF_{ISAT}	1.32	1.67	2.91	7.31
$SF_{ISAT\text{-}DAC}$	1.88	2.25	3.86	9.50

5. Conclusions

The use of DAC and ISAT for efficient simulations with complex chemical kinetics was explored for PaSR for methane/air combustion and HCCI combustion for iso-octane/air. It was found that DAC expedites the reaction sub-step in the operator-splitting scheme through local skeletal reduction using the DRG method, whereas ISAT expedites the calculations by reducing the number of direct ODE integrations through tabulating and re-using the solutions. Neither of the methods requires pre-processing or pre-tabulation of sample compositions and can facilitate the use of detailed chemistry in CFD with effective error control. ISAT was found to be more efficient than DAC for simulations where compositions can be frequently retrieved from the table. A speedup factor of up to about 1000 in the reaction sub-step was achieved for a premixed PaSR with good accuracy in temperature and species concentrations. It is expected that ISAT is most effective for simulations of statistically steady state flames with moderate sized mechanisms that contain

less than about 50 species. In contrast, the performance of DAC is mostly independent of the nature of the combustion simulations, e.g., steady or unsteady; premixed or non-premixed. The efficiency of DAC increases with the mechanism size, as such DAC is particularly suitable for combustion simulations with large mechanisms. A speedup factor of about 30 was achieved for HCCI combustion of a lean iso-octane/air mixture with good agreements in the histories of temperature and species concentrations.

An ISAT-DAC method that combines DAC and ISAT was developed for highly efficient CFD simulations with detailed chemistry. ISAT-DAC inherited the advantages in both ISAT and DAC to efficiently solve combustion problems with complex chemistry. The number of expensive direct ODE integrations is reduced by tabulating and re-using the solutions; and the necessary ODE integrations are expedited by the use of locally valid small skeletal mechanisms. It is demonstrated that the incurred errors in temperature and species concentrations are well controlled in ISAT-DAC. The use of DAC can improve the computational efficiency of ISAT by more than 30% as demonstrated in a non-premixed PaSR of methane/air. With the same level of computational efficiency, compared with stand-alone ISAT, ISAT-DAC significantly improved the accuracy in the predicted *NO* concentration.

Acknowledgments

The work by T. Lu is supported by the Chemical Sciences, Geosciences and Biosciences Division, Office of Basic Energy Sciences, Office of Science, U.S. Department of Energy, under Grant DE-FG02-12ER16345.

References

[1] Law, C. K., Proc. Combust. Inst. 31 (1) (2007) 1-29.
[2] Marchuk, G. I. in: *On the theory of the splitting-up method*, Proceedings of the 2nd Symposium on Numerical Solution of Partial Differential Equations, SYNSPADE, University of Maryland, May 11-15, 1970; Academic Press: University of Maryland, 1970; pp 469-500.
[3] Yanenko, N. N., The Method of Fractional Steps, Springer-Verlag, New York, 1971.
[4] Knio, O. M., Najm, H. N., Wyckoff, P. S., J. Comput. Phys. 154 (1999) 428-467.
[5] Sportisse, B., J. Comput. Phys. 161 (2000) 140-168.
[6] Ropp, D. L., Shadid, J. N., Ober, C. C., J. Comput. Phys. 194 (2004) 544-574.
[7] Singer, M. A., Pope, S. B., Najm, H. N., Combust. Theory Model. 10 (2) (2006) 199-217.
[8] Strang, G., SIAM J. Numer. Anal. 5 (3) (1968) 506-517.
[9] Schwer, D. A., Lu, P., Green, W. H., Semiao, V., Combust. Theory Model. 7 (2) (2003) 383-399.
[10] Ren, Z., Pope, S. B., J. Comput. Phys. 227 (2008) 8165-8176.
[11] Lu, T. F., Law, C. K., Proc. Combust. Inst. 30 (2005) 1333-1341.
[12] Lu, T. F., Law, C. K., Combust. Flame 146 (3) (2006) 472-483.
[13] Pepiot-Desjardins, P., Pitsch, H., Combust. Flame 154 (1-2) (2008) 67-81.
[14] Liang, L., Stevens, J. G., Farrell, J. T., Proc. Combust. Inst. 32 (2009) 527-534.
[15] Niemeyer, K., Sung, C., Raju, M., Combust. Flame 157 (9) (2010) 1760-1770.
[16] Sun. W, C. Z., Gou. X, Ju. Y, , in: *6th National Combustion Meeting of the U.S. Sections of the Combustion Institute, Paper# 23F3*, 2009.
[17] Tosatto, L., Bennett, B. A. V., Smooke, M. D., Combust. Flame 158 (2011) 820-835.
[18] Nagy, T., Turanyi, T., Combust. Flame 156 (2009) 417-428.
[19] Bodenstein, M., Lind, S. C., Z. Phys. Chem. 57 (1906) 168-175.
[20] Smooke, M. D., Reduced Kinetic Mechanisms and Asymptotic Approximations for Methane-Air Flames, Springer, Berlin, 1991.
[21] Keck, J. C., Gillespie, D., Combust. Flame 17 (1971) 237-241.
[22] Keck, J. C., Prog. Energy Combust. Sci. 16 (2) (1990) 125-154.
[23] Lam, S. H., Goussis, D. A., Int. J. Chem. Kinet. 26 (4) (1994) 461-486.
[24] Maas, U., Pope, S. B., Combust. Flame 88 (3-4) (1992) 239-264.
[25] Pope, S. B., Maas, U., in: *FDA 93-11*, Cornell University, 1993.
[26] Ren, Z. Y., Pope, S. B., Proc. Combust. Inst. 30 (2005) 1293-1300.
[27] Ren, Z. Y., Pope, S. B., Vladimirsky, A., Guckenheimer, J. M., J. Chem. Phys. 124 (11) (2006).
[28] Gorban, A. N., Karlin, I. V., Chem. Eng. Sci. 58 (21) (2003) 4751-4768.
[29] Al-Khateeb, A. N., Powers, J. M., Paolucci, S., Sommese, A. J., Diller, J. A., Hauenstein, J. D., Mengers, J. D., J. Chem. Phys. 131 (02) (2009) 1-19.
[30] Chen, J.-Y., Kollmann, W., Dibble, R. W., Combust. Sci. Technol. 64 (1989) 315-346.

[31] Turanyi, T., Comput. Chem. 18 (1994) 45-54.
[32] Christo, F. C., Masri, A. R., Nebot, E. M., Pope, S. B., Proc. Combust. Inst. 26 (1996) 43-48.
[33] Pope, S. B., Combust. Theory Model. 1 (1) (1997) 41-63.
[34] Lu, L., Pope, S. B., J. Comput. Phys. 228 (2) (2009) 361-386.
[35] Tonse, S. R., Moriarty, N. W., Brown, N. J., Frenklach, M., Isr. J. Chem. 39 (1) (1999) 97-106.
[36] Goldin, G. M., Ren, Z., Zahirovic, S., Combust. Theory Model. 13 (2009) 721-739.
[37] Aceves, S. M., Flowers, D. L., Westbrook, C. K., Smith, J. R., Dibble, R. W., Christensen, M., Pitz, W. J., Johansson, B. in: *A multi-zone model for prediction of HCCI combustion and emissions*, 2000; 2000.
[38] Babajimopoulos, A., Assanis, D. N., Flowers, D. L., Aceves, S. M., Hessel, R. P., Internat. J. Engine Res. 6 (2005) 497-512.
[39] Liang, L., Stevens, J. G., Raman, S., Farrell, J. T., Combust. Flame (2009) 527-534.
[40] Shi, Y., Liang, L., Ge, H. W., Reitz, R. D., Combust. Theory Model. 14 (2010) 69-89.
[41] Contino, F., Jeanmart, H., Lucchini, T., D'Errico, G., Proc. Combust. Inst. 33 (2011) 3057-3064.
[42] Yang, H., Ren, Z., Lu, T., Goldin, G. M., Combust. Theory Model. (2012).
[43] Haworth, D. C., Prog. Energy Combust. Sci. 36 (2) (2010) 168-259.
[44] Ren, Z., Goldin, G. M., Hiremath, V., Pope, S. B., Combust. Theory Model. 15 (2011) 827-848.
[45] Wang, H., Pope, S. B., Proc. Combust. Inst. 33 (2011) 1319-1330.
[46] Luo, Z., Lu, T., MacIaszek, M. J., Som, S., Longman, D. E., Energy and Fuels 24 (12) (2010) 6283-6293.
[47] Smith, G. P., Golden, D. M., Frenklach, M., Moriarty, N. W., Eiteneer, B., Goldenberg, M., Bowman, C. T., Hanson, R. K., Song, S., Gardiner, W. C., Lissianski, V. V., Qin, Z. http://www.me.berkeley.edu/gri_mech/. http://www.me.berkeley.edu/gri_mech/
[48] Luo, Z., Lu, T., Liu, J., Combust. Flame 158 (7) (2011) 1245-1254.
[49] Wang, H., You, X., Joshi, A. V., Davis, S. G., Laskin, A., Egolfopoulos, F., Law, C. K. USC Mech Version II. High-Temperature Combustion Reaction Model of H2/CO/C1-C4 Compounds. http://ignis.usc.edu/USC_Mech_II.htm
[50] Yao, M., Zheng, Z., Liu, H., Prog. Energy Combust. Sci. 35 (5) (2009) 398-437.
[51] Curran, H. J., Gaffuri, P., Pitz, W. J., Westbrook, C. K., Combust. Flame 129 (3) (2002) 253-280.
[52] Caracotsios, M., Stewart, W. E., Comput. Chem. Eng. 9 (1985) 359-365.